Impact of climate change on snowpack in the Pyrenees: Horizontal spatial variability and vertical gradients

López-Moreno, J.I.; Goyette, Stéphane; Beniston, Martin

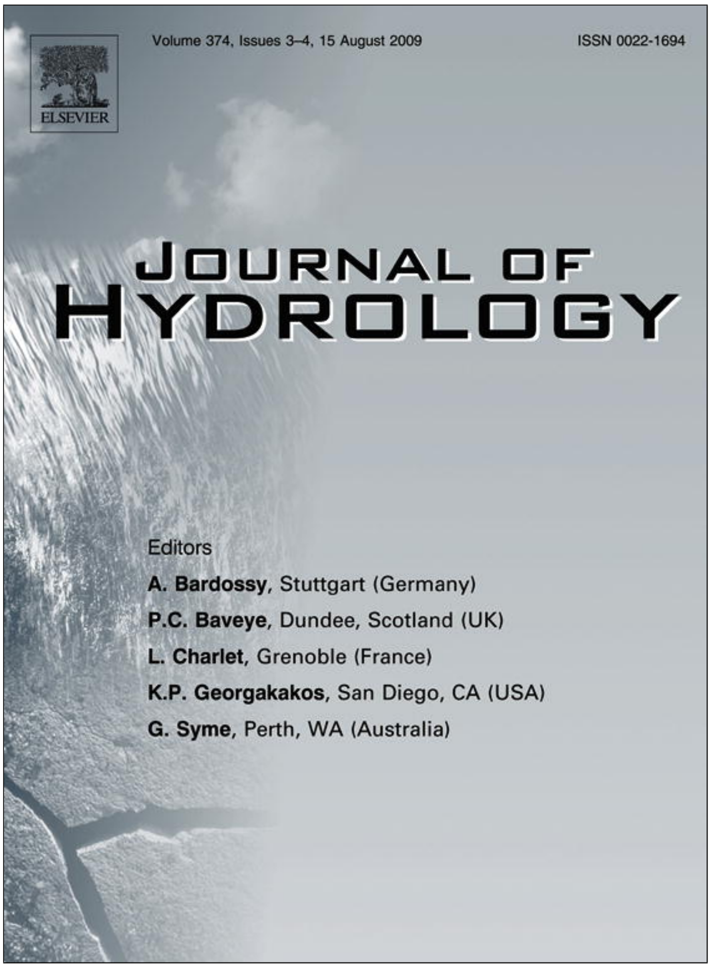
Volume 374, Issues 3–4, 15 August 2009
ISSN 0022-1694
ELSEVIER
JOURNAL OF
HYDROLOGY
Editors
A. Bardossy, Stuttgart (Germany)
P.C. Baveye, Dundee, Scotland (UK)
L. Charlet, Grenoble (France)
K.P. Georgakakos, San Diego, CA (USA)
G. Syme, Perth, WA (Australia)

Journal of Hydrology 374 (2009) 384–396

Contents lists available at ScienceDirect

Journal of Hydrology

journal homepage: www.elsevier.com/locate/jhydrol

Impact of climate change on snowpack in the Pyrenees: Horizontal spatial variability and vertical gradients

J.I. López-Moreno [a,*], S. Goyette [b], M. Beniston [b]

[a] Instituto Pirenaico de Ecología, CSIC, Campus de Aula Dei, P.O. Box 202, Zaragoza 50080, Spain
[b] Climatic Change and Climate Impacts Group, University of Geneva, Batelle/D, 7 Chemin de Drize CH-1227, Carouge (Geneva), Switzerland

ARTICLE INFO

Article history:
Received 17 July 2008
Received in revised form 20 May 2009
Accepted 27 June 2009

This manuscript was handled by K. Georgakakos, Editor-in-Chief, with the assistance of Gunter Bloschl, Associate Editor

Keywords:
Climate change
Snow
Greenhouse gases emission scenarios (SRES)
Spatial variability
Altitudinal gradients
Pyrenees

SUMMARY

In this study, snowpack series are modeled across the Pyrenees using data derived from the HIRHAM Regional Climate Model for both the control period (1960–1990) and two emission scenarios (SRES B2 and A2) by the end of the 21st century (2070–2100). A comparison of future and control simulations enables us to quantify the expected change in snowpack for the next century. Snow simulations are performed on 20 Regional Climate Model (RCM) grid points over the Pyrenees, covering the entire north–south and east–west transects; data were downscaled for four different altitudinal levels (1500, 2000, 2500, and 3000 m a.s.l.). This procedure yields a relatively complete picture of the expected impacts of climate change in the Pyrenees, covering horizontal spatial variability as well as altitudinal gradients. According to the HIRHAM model projections following different greenhouse gas emission scenarios, the thickness and duration of snowpack in the Pyrenees will decrease dramatically over the next century, especially in the central and eastern sectors of the Spanish Pyrenees. The magnitude of these impacts will follow a marked altitudinal gradient: the maximum accumulated snow water equivalent may decrease by up to 78%, and the season with snow cover may be reduced by up to 70% at 1500 m a.s.l. The magnitude of the impacts decreases rapidly with increasing altitude; snowpack characteristics will remain largely similar in the highest sectors. The decline of the snowpack would be reduced by half if a medium–low emission scenario was considered (B2) instead of the medium–high concentrations of greenhouse gas assumed in the A2 scenario.

Introduction

As snow and ice respond rapidly to slight variations in precipitation and temperature (Nesje and Dahl, 2000; Carrivick and Brewer, 2004; López-Moreno and Vicente-Serrano, 2007), the cryosphere is the most sensitive element of the Earth System to climate change (Marty, 2008). Focusing on snow, many studies have attempted to assess the distribution and magnitude of seasonal snowpack under a warmer climate. This is an important investigation because snow cover exerts a strong control over ecology, agriculture, the availability of water resources, the operation of a diverse range of economic activities, and associated risks in mountainous and high-latitude regions (Beniston, 1997; Barnett et al., 2005).

With the exception of some areas for which climate models project increasing precipitation (i.e., areas located at very high-latitudes, where increased snow is expected; Räisanen, 2008), most previous studies highlight the likelihood over the coming decades of a sharp decrease in accumulated snow, shortening of the snow cover season, and a decreasing and earlier spring freshet (Rasmus et al., 2004; Dankers and Christensen, 2005; Keller et al., 2005; Merritt et al., 2006; Hantel and Hirtl-Wielke, 2007; Mellander et al., 2007).

Despite the overall similarity of previous findings, it is evident that further research is required on this topic to obtain a more complete picture of the global-scale impacts of climate change, as many mountain sectors remain poorly studied. Moreover, new methodological approaches and case studies are needed to address the high degree of topographic heterogeneity in mountainous areas and the generally sparse nature of meteorological data available for such regions, as these factors make it difficult to handle spatial variability and they enhance the level of uncertainty in assessments of climate change compared with studies that focus on flat regions (López-Moreno et al., 2008a).

This study aims to evaluate the potential impact of climate change on snowpack across the Pyrenees, a mountain range running in the northeast of the Iberian Peninsula. The focus is on changes in total accumulated snow water equivalent (ASWE) and duration of snowpack at the surface (DSP). Changes will be assessed by comparing snowpack simulations for the control period (1960–1990) and these of two contrasted greenhouse emission

* Corresponding author. Tel.: +34 976 716040; fax: +34 976 716039.
E-mail address: nlopez@ipe.csic.es (J.I. López-Moreno).

0022-1694/$ - see front matter © 2009 Elsevier B.V. All rights reserved.
doi:10.1016/j.jhydrol.2009.06.049

scenarios for the period (2070–2100). Special attention will be paid to detect spatial variability in the magnitude of the change in both: horizontal variability and altitudinal gradients.

In addition to important ecological factors that depend on snowpack variability, climate change in this region could have important socio-economic implications, mainly due to: (i) the importance of snowmelt for the availability and management of water resources in the semiarid and highly populated Ebro Valley (López-Moreno and García-Ruiz, 2004), and (ii) the high dependence of the regional economy on winter tourism, which represents one of the main revenue streams for the region (Lasanta et al., 2007).

López-Moreno et al. (2008a) highlighted the likelihood of important shifts in precipitation and temperature within the Pyrenees over the coming decades. The authors also used a surface energy balance model (SEBM) to simulate the snow surface at a single location under current and projected future climatic conditions. Results showed the marked sensitivity of Pyrenean snowpack duration and thickness to shifts in temperature, precipitation, and solar radiation (López-Moreno et al., 2008b). As one of the most important drivers of the SEBM was found to be temperature, and the nine different Regional Climate Models (RCMs) used in the study indicated a marked spatial variability across the Pyrenees in the evolution of precipitation, it was assumed that changes in snowpack under future climatic conditions will be subject to strong vertical gradients and show contrasting magnitudes across north–south and Mediterranean–Atlantic transects.

In this study, the lack of long-term detailed meteorological records for the region prevented the use of approaches commonly employed for snow studies based on comparisons of simulated snowpack with available meteorological records, with further simulations using modified series yielding projected future conditions; in other words, perturbing the observations using the so-called delta method (e.g., Keller et al., 2005; Mellander et al., 2007; López-Moreno et al., 2008b; Uhlmann et al., 2009). The use of snow water equivalent (SWE) provided by GCMs or by RCMs outputs, or these by a SEBM driven by outputs generated by the latter is also made difficult because their spatial resolution is too coarse (latitude/longitude resolution generally coarser than 0.44°) to capture the heterogeneity of rugged mountainous terrain.

To address these limitations in the present study, the seasonal evolution of snowpack is simulated at 20 individual points covering the entire Pyrenees, each of them representing average conditions over a surface area typical of a RCM employed during the EU PRUDENCE project, 50 km^2 (Christensen et al., 2002). Snowpack series are simulated by running a SEBM model (GRENBLS, Keller et al., 2005) with climatic inputs provided by the HIRHAM Regional Climate Model (Christensen et al., 1998) for both the control situation (1960–1990) and future (2070–2100) scenarios. Prior to the analysis, climatic variables are spatially downscaled for four altitudinal levels, i.e., 1500, 2000, 2500, and 3000 m a.s.l., and daily series are disaggregated into hourly data.

The following sections present and describe the procedures and assumptions adopted in downscaling the climatic data and obtaining hourly data from daily series, consider the reliability of HIRHAM data and snow-derived series, and outline the projected changes in snowpack for the region during the 21st century.

Study area

The study area includes both the French and Spanish sides of the Pyrenees, and is bounded by the Mediterranean Sea to the east and the Atlantic Ocean to the west (Fig. 1). Altitude ranges from 300 m to more than 3000 m a.s.l. A total of 5768 km^2 of land area lies above 1500 m, 3523 km^2 of them are above 2000 m, 735 km^2 above 2500 m, and 5 km^2 above 3000 m.

The climate of the Pyrenees is subject to an eastward transition from Atlantic to Mediterranean conditions. Moreover, macro-relief introduces a noticeable variability to the distributions of precipitation and temperature. The Foehn effect is frequently observed in the area, wet air masses are lifted up in northern slopes leading to drier and warmer conditions southward, a process that enhances noticeably the differences in precipitation between the northern and southern slopes, and imposing higher temperatures on the southern side. In the Central Ebro Depression, the average annual precipitation is approximately 300 mm and the average annual temperature is 13–15 °C. In the mountains themselves, annual precipitation exceeds 600 mm, reaching 2000 mm at the highest divides. Most of the annual precipitation falls during the cold season (December–March) in the Atlantic areas and during spring and autumn (April–June and September–November, respectively) in the Mediterranean regions. Summers are generally relatively dry in the Pyrenees, and are very dry in the Ebro Depression.

Various thermal gradients have been proposed by a number of authors. For the entire Pyrenean range, García-Ruiz et al. (1986) estimated an altitudinal gradient of 0.6 °C/100 m, and López-Moreno (2006) calculated a gradient of 0.63 °C/100 m. Based on these gradients, the annual 0 °C isotherm is confined to around

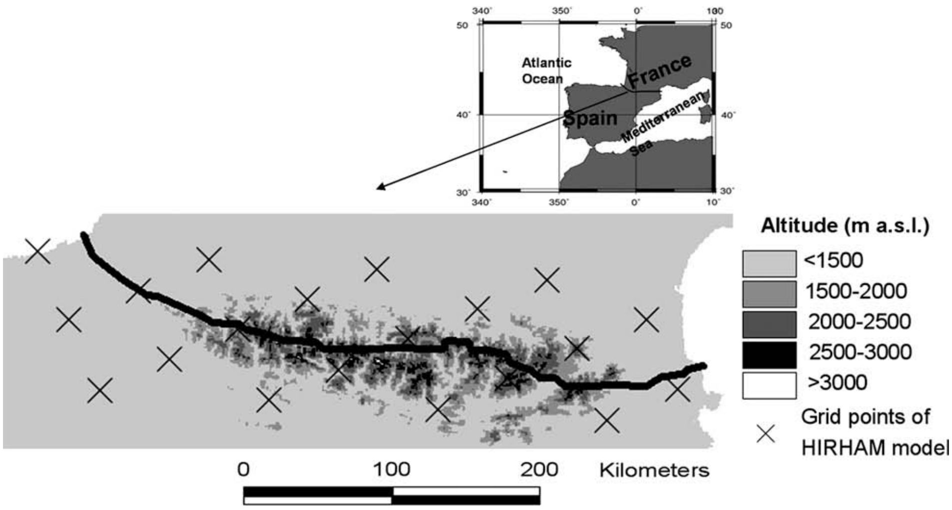

Fig. 1. Map of the study area. Crosses indicate the grid points of the HIRHAM model used to simulate snowpack.

2900 m (Chueca-Cía et al., 2003). Between November and April, the 0 °C isotherm is located at approximately 1600–1700 m a.s.l. (García-Ruiz et al., 1986), representing the level above which snow accumulates over a long period.

Data and experimental setup

Snow model

In this study we used a SEBM including an explicit representation of the snowpack computed on the basis of a snow module of an intermediate complexity such as that included in GCMs and in RCMs. This SEBM is termed GRENBLS (Ground Energy Balance for natural Surfaces), driven by hourly atmospheric data. Previous studies have demonstrated genuine skill in reproducing many aspects of the energy fluxes and evolution of alpine snowpacks (Keller et al., 2005; Keller and Goyette, 2005; Uhlmann et al., 2009). The later references provide a full description of the model characteristics. The application of GRENBLS and the obtained error estimators for simulating snowpack in the Pyrenees can be found in López-Moreno et al. (2008b).

A number of different numerical modeling approaches have been employed for the simulation of snow cover, ranging from simplified degree-day melt models (e.g., Anderson, 1973), to single (e.g., Outcalt et al., 1975) and multi-layer (e.g., Anderson, 1976; Brun et al., 1989; Tuteja and Cunnane, 1997) energy balance models. An evaluation of snow models undertaken as part of the Snow Model Intercomparison Project (SnowMIP) revealed that single-layer models are able to provide adequate representations of SWE over a range of snow cover climates (Etchevers et al., 2003), providing realistic results even when compared with relatively complex multi-layer models (e.g., Brown et al., 2006).

GRENBLS is a physically-based model driven by hourly input data of screen air temperature, T_a (K), dew point temperature, T_d (K), anemometer-level wind magnitude, W_s (m s^{-1}), precipitation, P (mm s^{-1}), surface pressure, p_{sfc} (hPa), and incident solar radiation ($K\downarrow$). The model was ran considering an explicit underlying multi-layer soil (of "medium–coarse texture") of 1 m depth covered at the surface by 70% of low vegetation (snow mask of 3 cm), 30% of bare soil, and a distinct snow layer. The model computes the radiative fluxes from cloudiness data and the surface turbulent sensible and latent fluxes. The bulk heat and moisture transfer coefficients are parameterized according to Benoît (1977) based on the Monin–Obukov similarity theory. Surface temperature, soil moisture, and snow mass are prognostic variables. The energy budget also considers the energy change associated with the melting of frozen soil moisture and snow. The temperature of the snowpack is computed in a prognostic manner via heat storage using a force-restore method (e.g., Stull 1988, chapter 7; McFarlane et al., 1992). Precipitation is considered as solid if T_a is less than that of the triple point of water. Liquid precipitation on a snowpack induces snowmelt, and the melt water enters directly into the soil in liquid form.

Snow is modeled as an evolving one-layer pack characterized by temperature T_{snow} (K), mass M_{snow} (kg m^{-2}), and density ρ_{snow} (kg m^{-3}). The surface energy budget is computed over the snow cover at each model time step. The radiative and turbulent fluxes are computed first, followed by heat storage in the snowpack; if the latter value is positive and the snow temperature is below the melting point, the excess energy is first used to raise the temperature of the pack. Once the temperature reaches the melting point, any additional excess energy is the used to melt the snow. The age effect of the snow on snow density has been adopted following the ideas of Verseghy (1991). The snow density of the bulk snow layer increases exponentially with time from the fresh-fallen snow value, $\rho_{snow,min}$ = 100 kg m^{-3}, to a maximum of $\rho_{snow,max}$ = 300 kg m^{-3}. In a similar manner, changes in snow albedo that accompany snow aging are parameterized as a time-decay function from an initial fresh snow albedo of 0.80.

Freshly-fallen snow has a fixed density of 100 kg m^{-3}. In a similar manner, changes in snow albedo that accompany snow aging are parameterized as a time-decay function from an initial fresh snow albedo of 0.80.

GRENBLS also incorporates total cloudiness as an input parameter (herein referred to as "C"). If solar radiation is prescribed from observations, cloudiness influences only the downward infrared thermal radiation at the surface; otherwise clouds contribute to deplete downward solar radiation by decreasing the direct and increasing the overall diffuse solar flux. Clouds influence the intensity of the direct and diffuse downward solar and infrared radiation at the surface. Under clear sky, solar radiation received at the surface, $K_o\downarrow$, is computed as a function of the eccentricity of the Earth's orbit around the sun, the cosine of the zenith angle, the latter is determined on the basis of the latitude of the station, the solar declination, and the hour angle, and on a transmissivity function. The Rayleigh and Mie diffusion processes are also considered. Under cloudy sky, the solar radiation is further depleted and the parameterization is implemented according to the ideas of Nunez et al. (1971). This considers low-, mid- and high-level cloud amounts. Two effects are considered: (1) the attenuation of the downward solar radiation by reflection and by dispersion processes and, (2) the downward reflection of the fraction of the solar radiation once reflected by the ground. The total cloud transmittance, Ψ_C, assuming a uniform cloudiness in each layer, is given by the product of the layer transmittance. The transmissivity of the ith layer of clouds is then given by:

$$\Psi_{C_i} = 1 - (1 - t_1)C_i$$

where the ith layer contains a fraction C_i of clouds of transmittance t_i. Consequently, the global solar radiation reaching the surface, $K\downarrow$, is parameterized as follows:

$$K\downarrow = K_o K\downarrow = K_o\downarrow \Psi_C = K_o\downarrow \Pi \Psi_C(1 - \alpha\alpha_C C)$$

where α is the surface albedo and α_C the cloud-base albedo, and C is the sum of low-, mid-, and high-level cloud amounts.

At temperatures characteristic of the Earth's surface, about 70% of the energy in the black-body spectrum lies outside the waveband of the atmospheric window (8–14 μm), whereas the atmosphere neither absorbs nor radiates those wavebands within the window. At all other wavelengths, the atmosphere is considered to behave as a black-body. Hence, 70% of the outgoing longwave radiation is absorbed and re-radiated downwards at wavelengths outside of the window; that is, the atmospheric emissivity $\varepsilon_a = \frac{L_o^\downarrow}{\sigma T_{air}^4}$ is 0.7, where $L_o^\downarrow$ is the cloudless sky flux density and σ the Stefan–Boltzmann constant. Paltridge and Platt (1976) state that the downward energy flux density (0.7–1), $\varepsilon_c \sigma T_c^4$, may generally be used with a mean value of 60 W m^{-2}, where ε_c and T_c are the cloud emissivity and temperature, respectively. Clouds affect the flux density at the ground by contributing longwave radiation within the window:

$$L\downarrow = L_o^\downarrow + (1 - 0.7)\varepsilon_c \sigma T_c^4 C \tag{1}$$

where $0 \leqslant C \leqslant 1$.

Input data scaling

Control (1960–1990) and future climate (2070–2100) data were obtained from the outputs of the Danish Meteorological Institute (DMI) HIRHAM RCM. This RCM was used for a dynamical downscaling of the Atmosphere–Ocean General Circulation Model

(AOGCM) HadAM3H for the European continent to a spatial resolution of 0.5° latitude/longitude, i.e., roughly 50 km (Christensen et al., 1998). RCM outputs are made available on a daily basis, available for download from the Web site of the EU-PRUDENCE project: http://prudence.dmi.dk. The present study required information on maximum temperature (T_{max}), minimum temperature (T_{min}), precipitation (P), dew point temperature (T_d), atmospheric surface pressure (p_{sfc}), wind speed (W_s), and cloudiness (C). Incident solar radiation is computed in combination with the cloud data.

The models were run for a control period (1961–1990) and two contrasting future scenarios (2070–2100) of greenhouse gas emissions (SRES A2 and B2) based on different hypotheses defined by the Intergovernmental Panel for Climate Change (IPCC, 2007; Nakicenovic et al., 1998) related to economic and demographic behavior by 2100. B2 describes a world in which the emphasis is on local solutions to economic, social, and environmental sustainability, in a world where global population increases continuously (at a rate lower than that in A2) and with intermediate levels of economic development. A2 is characterized by much higher emissions of greenhouse gases, and provides a closer match with future trends based on gas concentrations measured over the past decade (IPCC, 2007).

The degree of reliability in reproducing observed climate in the Pyrenees during the control period was assessed for six different RCMs that belong to the PRUDENCE dataset. The analysis revealed that the HIRHAM RCM provides one of the most reliable simulations for temperature and precipitation throughout the year. Biases compared with observed data lie within 1 °C for temperature (0.26 °C and 0.71 °C for maximum and minimum winter – December–February – and 0.1 °C and 0.7 °C for spring – March–May – temperatures, respectively) and 20% for precipitation (10% and 17% for winter and spring temperature, respectively). These values are in line with the errors found for Europe in previous quality assessments of RCMs (Giorgi et al., 2004a; Déqué et al., 2005). Moreover, HIRHAM model has been able to appropriately reproduce several characteristics of daily precipitation in the study area, such as the number of rainy days, precipitation intensity and frequency of heavy precipitation events (López-Moreno and Beniston, 2009).

Model outputs are given for grid points at the centre of each 50 × 50 km grid cell. Because spatial resolution does not enable a realistic representation of the climatic variability of the region, the daily altitudinal gradients of simulated temperature, precipitation, and dew point temperature were obtained by linear regression for the 20 grid cells that cover the Pyrenean surface. Whenever the correlation is statistically significant and the slope of the regression between a climatic parameter and altitude is known, it is possible to predict values for different altitudinal planes for each day. In this study, daily climatic values were downscaled for 1500, 2000, 2500, and 3000 m a.s.l by means of the application of daily elevation adjustment rates. As expected, daily linear regressions yielded slopes with marked day-to-day variability. Mean annual gradients (obtained from averaging daily gradients) for simulated temperature and precipitation were −0.61 °C/100 m and 41 mm/100 m, respectively, similar to the values of −0.63 °C/100 m and 46 mm/100 m obtained from observed data (López-Moreno, 2006). Determination coefficients (r^2) of the annual relationships between altitude and simulated mean temperature, precipitation, and dew point temperature were 0.92, 0.57, and 0.81, respectively, being statistically significant ($\alpha < 0.01$) in all three cases. Atmospheric pressure is adjusted to different altitudinal planes by applying the following barometric correction (Berberan-Santos et al., 1997):

$$p_{sfc} = p_{obs}\left(\frac{T_{air}}{T_{air} + \gamma\Delta z}\right)^{\frac{g}{R_d\gamma}} \tag{2}$$

where T_{air} is the observed temperature (K), p_{obs} is the atmospheric pressure (p_{sfc}) at the grid point altitude, Δz is the altitude difference, γ is a mean vertical lapse rate defined as −6.5 K/km, g is gravitational acceleration (9.81 m s^{-1}), and R_d is the specific gas constant for dry air (287.04 J kg^{-1} K^{-1}).

Given a lack of appropriate data and absence of clear altitudinal trends in simulated wind speed, we consider it invariant with altitude.

As GRENBLS employs hourly data as an input and RCMs usually provide outputs on a daily basis, HIRHAM climatic data are disaggregated into hourly series following the procedures and assumptions described below. For temperature data, a cosine function was adjusted to daily maximum and minimum temperature via the following analytical equation (see Jansson and Karlberg, 2004):

$$T_a(t) = T_{mean} - T_{amp}\cos\left(\frac{t - t_{ph}}{y_{cycle}}2\pi\right) \tag{3}$$

where t represents the time in hour, $T_a(t)$ is air temperature, T_{mean} is the mean daily temperature, T_{amp} is the daily amplitude in temperature ($T_{max} - T_{min}$), t_{ph} is the phase shift in air temperature (2400 when a diurnal cycle is assumed), and y_{cycle} is the air temperature cycle (24 h). Fig. 2 compares observed hourly data with data converted from daily-to-hourly using Eq. (3), based on information from an automatic weather station located in the Central Pyrenees. The strong agreement between the two series confirms the reliability of the procedure used.

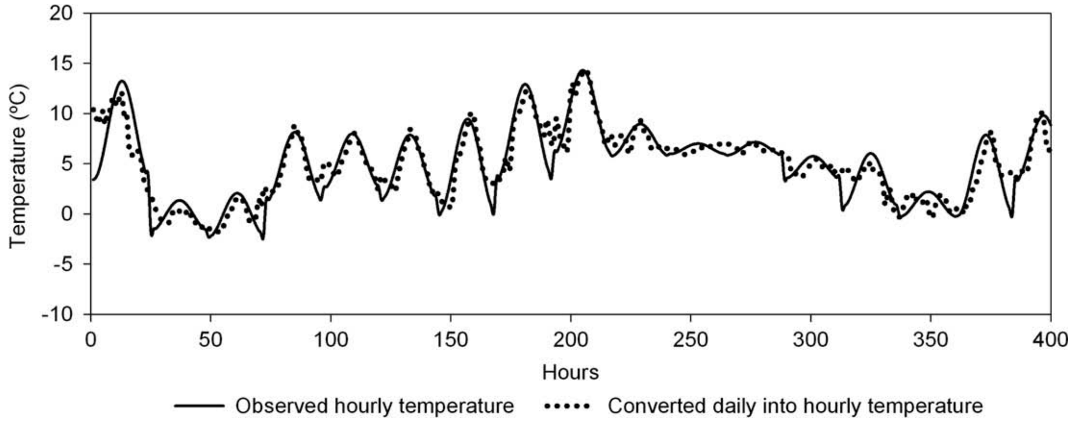

Fig. 2. Comparison of observed hourly data and daily-to-hourly converted data using a cosine function. Hourly information was measured by an automatic weather station located in the Central Pyrenees.

At each grid point, cloudiness (C), wind speed (W_s), and surface pressure (p_{sfc}) are assumed to change linearly from one day to the next, in an hourly fashion. Surface pressure (p_{sfc}) is then estimated for different iso-altitude planes via barometric correction (Eq. (2)), using temperature data disaggregated in hourly series with Eq. (3). Total daily precipitation was divided by 24 and shared equally throughout the day.

For a given moisture content in the atmosphere (specific humidity, q), relative humidity and dew point temperature (T_d) change with air temperature. It is therefore not convenient to

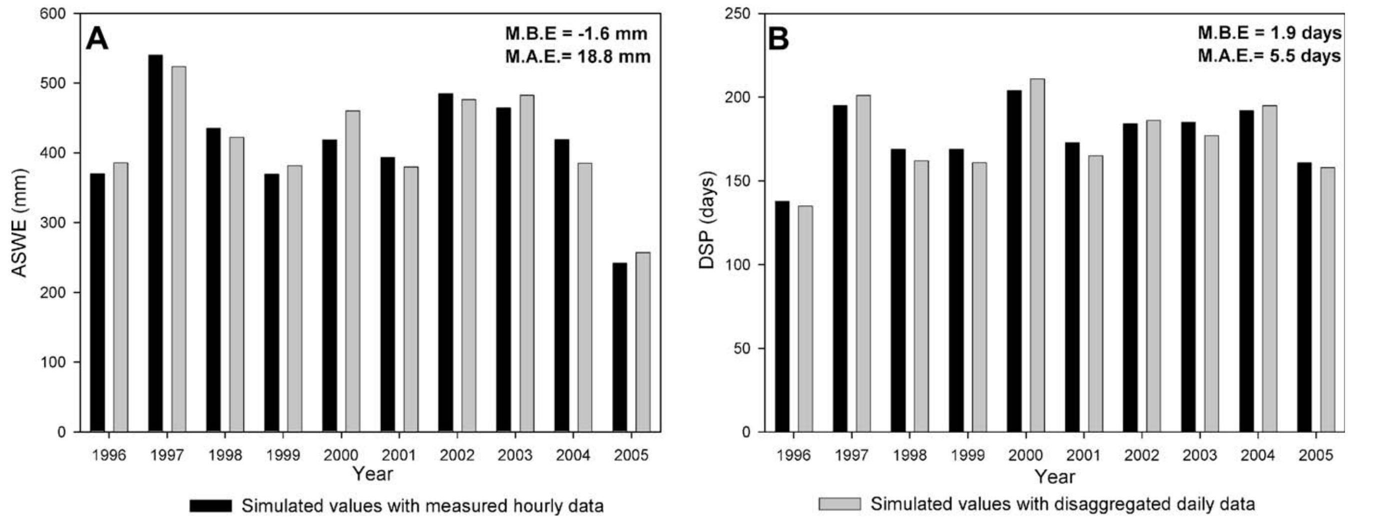

Fig. 3. (A) Annual accumulated snow water equivalent (ASWE) and (B) snowpack duration (DSP) simulated from observed (black) and disaggregated (grey) hourly data. M.B.E. is mean bias error and M.A.E. is the mean absolute error.

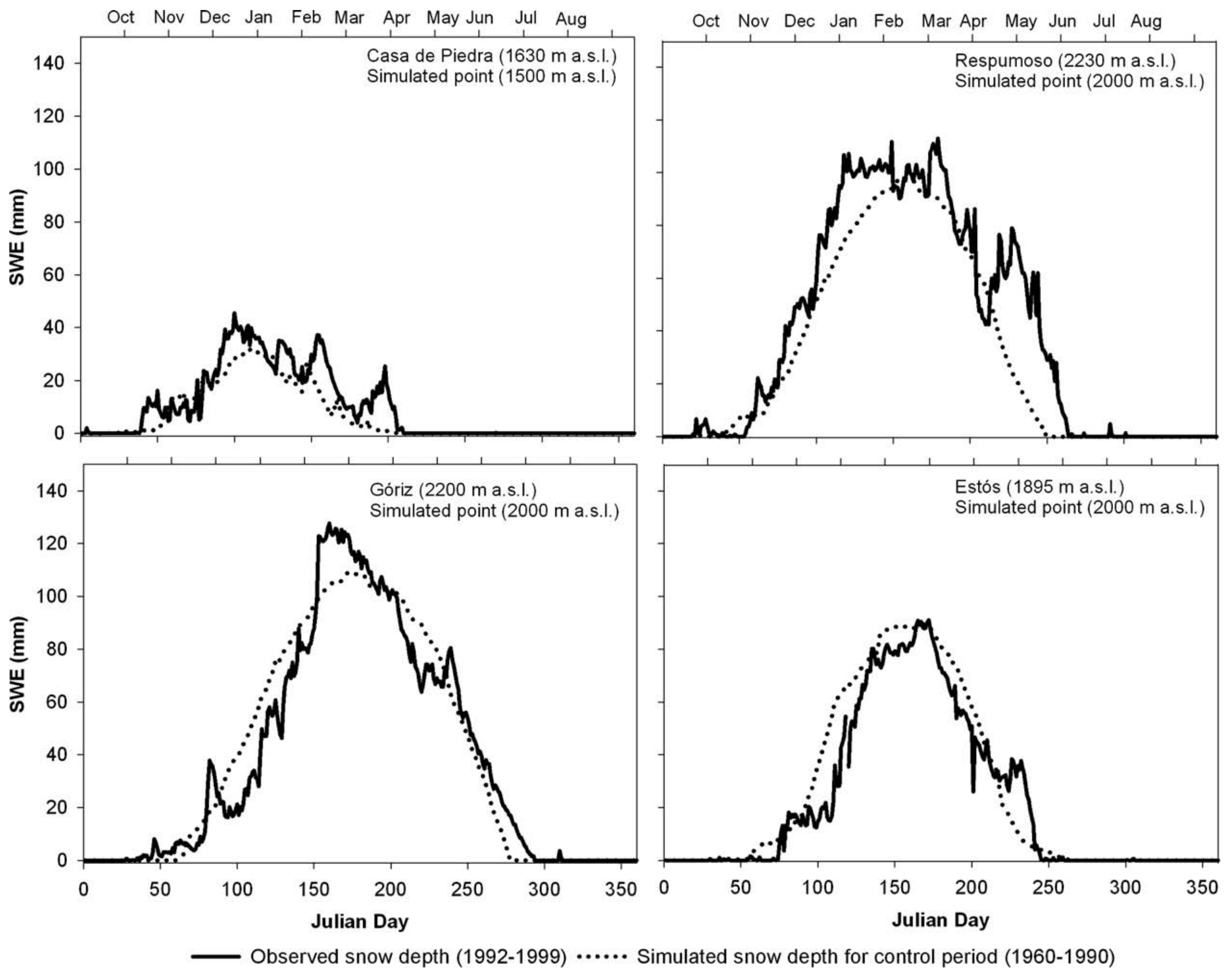

Fig. 4. Comparison of mean daily snow depth recorded in the 1990s at four locations and simulated snow series (control period) at the closest grid cell and altitudinal level.

linearly disaggregate T_d when air temperature shows a well-known daily cycle (simulated in this study with a cosine function, Eq. (3)). Thus, we followed the following steps:

1. T_d series were converted into specific humidity from temperature and surface pressure (p_{sfc}) data by obtaining vapor pressure (e) from Eq. (5).
2. Once calculated vapor pressure specific humidity (q) was derived from Eq. (6).
3. Specific humidity was then disaggregated hourly assuming a linear change from one day to the next.
4. Series of vapor pressure (e) and saturated vapor pressure (e_{sat}, Eq. (4).) were estimated hourly using the disaggregated specific humidity (Eq. (6)) and atmospheric surface pressure (p_{sfc}; Eq. (2)) that includes temperature disaggregated by using Eq. (3).
5. The hourly dew point temperature series were calculated (Eq. (8)) using series of relative humidity (from Eq. (7)) and temperature.

The following psychometric equations (Perry and Green, 1997; Shallcross, 1997) were used for the transformations explained above:

$$e_{sat} = 6.1078 * EXP\left(\frac{17.2693T_a}{T_a + 238.3}\right) \quad (4)$$

$$e = 6.1112 * EXP\left(\frac{17.7T_d}{T_d + 243.5}\right) \quad (5)$$

$$e = \frac{p_{sfc}}{\left(\frac{0.622}{q} - 0.378\right)} \quad (6)$$

$$H_r(t) = 100\left(\frac{e(t)}{e_{sat}(t)}\right) \quad (7)$$

$$T_d(t) = [112 + 0.9T_a(t)]\sqrt[8]{\frac{H_r(t)}{100}} + 0.1T_a(t) - 112 \quad (8)$$

In order to assess the uncertainty associated to disaggregate hourly from daily data, we used the meteorological record (1996–2006) of the Izas weather station. This is one of the few automatic weather stations located in the study area. Hourly data was converted into daily records, and then we applied the disaggregation procedure described in this section. Fig. 3 shows the annual accumulated snow water equivalent (ASWE) and the duration of snowpack (DSP) simulated with the observed and disaggregated hourly data. ASWE and DSP calculated using both kind of data exhibit very similar values, with −1.6 and 18 mm of mean bias error and absolute error for ASWE, and 1.9 days and 5.5 days, respectively, for DSP. Mean absolute error never exceeds 5% of the magnitude of the mean ASWE and MAE for the period 1996–2005, which confirms that disaggregation method is a reliable alternative when hourly data is not available.

Quantification of the impact of climate change on snowpack

GRENBLS is run using hourly T_a, T_d, P, p_{sfc}, W_s and C once disaggregated from daily HIRHAM data and subsequently scaled at different altitudinal planes over a control period (1960–1990) and SRES B2 and A2 (2070–2100). Outputs are SWE and snow depth series at hourly intervals at 20 points and at the four different altitudinal levels considered (1500, 2000, 2500 and 3000 m a.s.l.). Thus, results shown in this study are based on a total of 240 model simulations (20 points × 4 altitudes × 3 RCM simulations, i.e., one control and two scenarios). The snow series were then simplified into daily series considering the SWE and snow depth simulated at noon. The annual accumulated SWE and duration of snowpack were calculated from simulated series. Accumulated SWE (ASWE) is the sum of every positive change in SWE between consecutive days during a complete snow season, and duration of snowpack (DSP) represents the sum of recorded days in a given year with SWE above 5 mm. The mean values calculated for each grid point

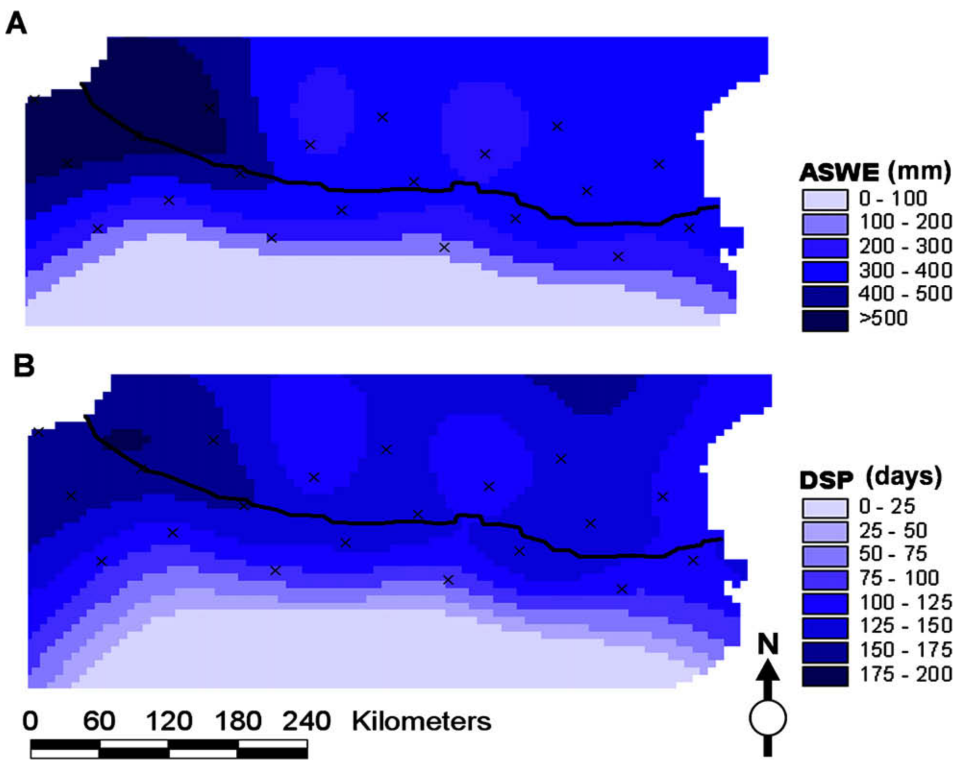

Fig. 5. Distributed mean accumulated snow water equivalent (A) and duration of snowpack (B) simulated using HIRHAM data for the Pyrenees during the control period at 2000 m a.s.l.

at the different iso-altitude planes for SRES B2 and A2 were subtracted from those obtained for control runs, enabling the quantification of the expected change in both parameters across the Pyrenees by the end of the 21st century. Point information was spatially interpolated for each altitudinal plane using splines with tension (Mitasova and Mitas, 1993) to obtain distribution maps showing the impact of climate change on ASWE and DSP. Moreover, average daily values over the 30 years of each simulation for the 20 grid points were averaged to obtain annual patterns and several indicators of snow accumulation and melting in the Pyrenees at different altitudes under current and future climate conditions.

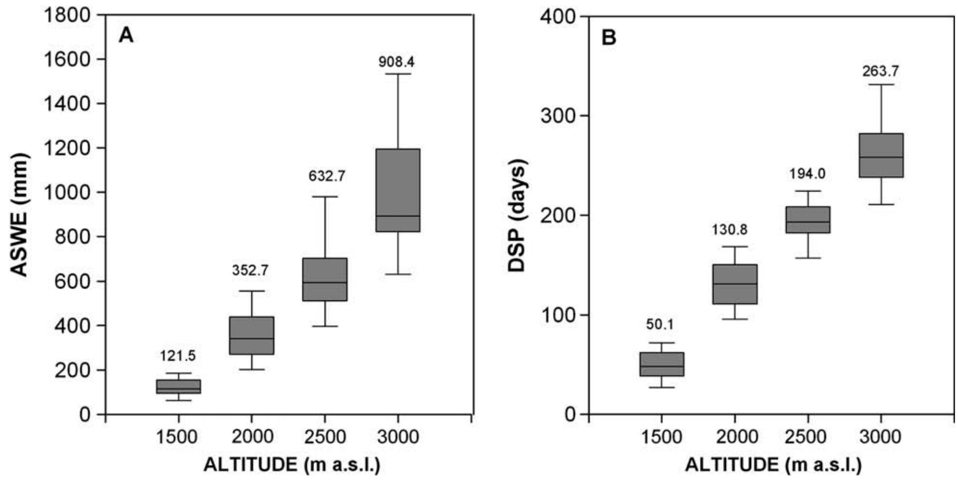

Fig. 6. Variability in accumulated snow water equivalent (A) and duration of snowpack (B) simulated for 20 grid points at four different altitudinal planes.

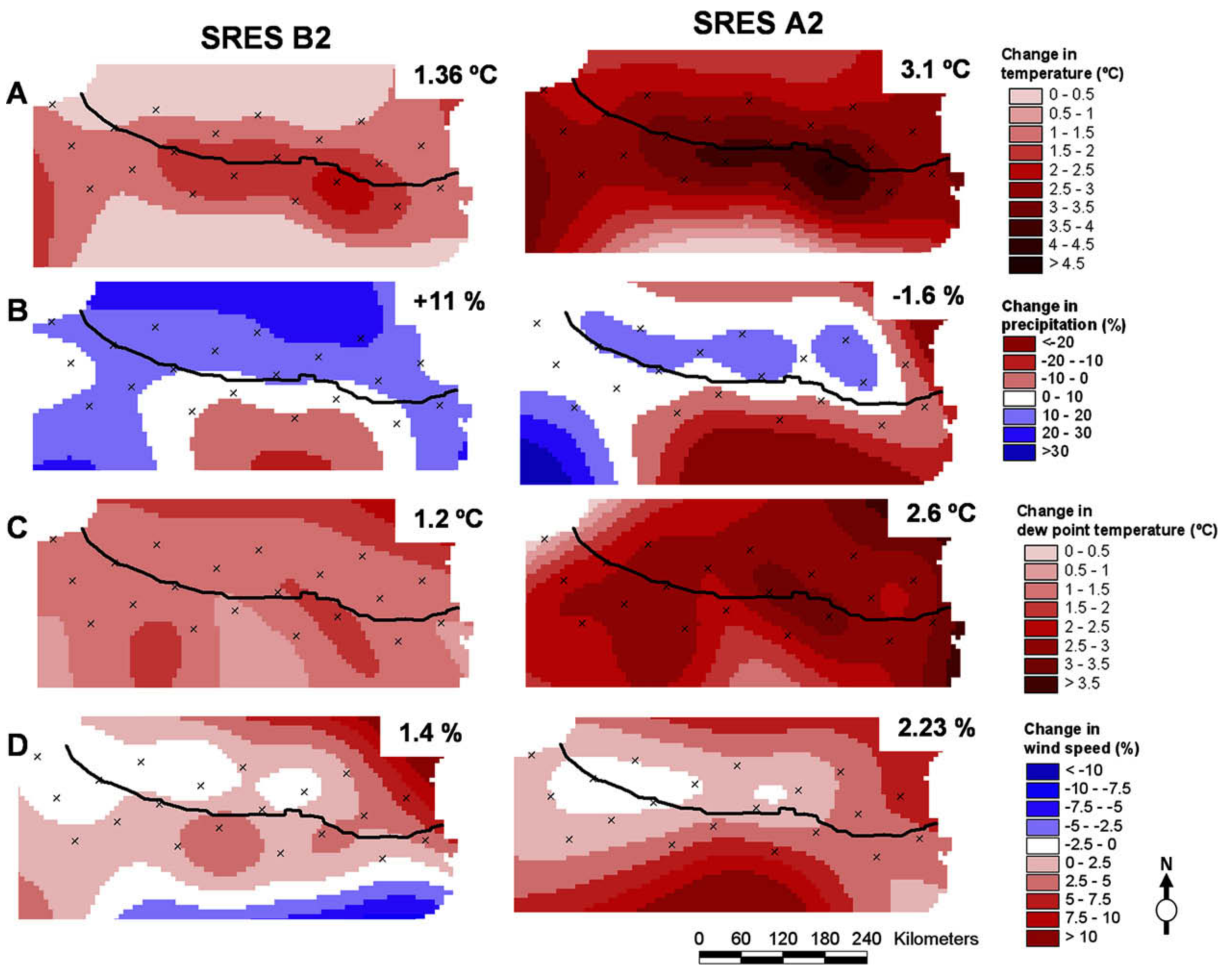

Fig. 7. Projected change (HIRHAM model, December–April period) by the end of the 21st century for some of the most influential variables on the snow energy balance under SRES B2 (left) and A2 (right): temperature (A), precipitation (B), dew point temperature (C), and wind speed (D).

Results

Simulated snowpack for the control period

Assessing the reliability of snow simulated using RCM data is a rather difficult exercise, as there exist only few records of observed snow depth in the study area and none of them corresponds with the control period. Moreover, observed snow depth at a given location is strongly affected by local conditions (aspect, wind drift processes, etc.), whereas data derived from RCMs reflect the mean conditions of a 50 × 50 km grid cell. To assess the capacity of simulated snowpack with an energy balance model based on HIRHAM data to reproduce Pyrenean snowpack and its spatial distribution, mean daily snow depth recorded at four locations in the 1990s are compared with simulated snow series at the closest grid cells and at the altitudinal plane closest to the location of the observed records (Fig. 4).

There is a rather good agreement in the overall snow depth and duration between the observed and the simulated snowpack despite some discrepancies on the short term. Thus, differences in simulated snowpack at 1500 and 2000 m a.s.l. are similar to those observed between Casa de Piedra and Respumoso. The simulations also reproduce the eastward decreasing trend in snowpack magnitude (e.g. Estós station: Fig. 4 bottom and right-hand panels); this trend arises from the lower winter precipitation under increasingly Mediterranean-type conditions.

Fig. 5 shows the distributed mean ASWE and DSP simulated using HIRHAM data for the Pyrenees at 2000 m a.s.l. for the control period. As the point data were interpolated, uncertainty in the predicted values increases markedly with increasing distance to simulated grid points. Fig. 6 shows the degree of variability among the 20 simulated grid points. Figs. 4 and 5 reveal a marked spatial variability and vertical gradients in both ASWE (max: 559.6 mm; min: 152.3 mm) and DSP (max: 169.2 days; min: 81.7 days). ASWE is larger and snowpack lasts longer on the northern slopes (French Pyrenees) than the south-facing ones. There also exists a trend toward greater and more prolonged accumulation of SWE in areas exposed to Atlantic climatic conditions (westward) compared with areas influenced by Mediterranean conditions (eastward).

The boxplots in Fig. 6 reveal the high sensitivity of snowpack to altitude. On average, ASWE is 121.5 mm at 1500 m a.s.l., three times as much (352.7 mm) at 2000 m, 632.7 at 2500 m, and 908.4 mm at 3000 m. The duration of snowpack shows a marked increase with altitude, ranging from an average of 50.1 days at 1500 m to 263.7 days at 3000 m a.s.l. Large variability in snow accumulation and snowpack duration is observed within individual iso-altitude planes (Fig. 5).

Projected climate change for the Pyrenees

Fig. 7 shows the change projected by the HIRHAM model by the end of the 21st century during the period December–April for some of the most important variables that influence the snow energy balance: temperature, precipitation, dew point temperature, and wind speed (López-Moreno et al., 2008b). Boxplots in Fig. 8 shows the degree of variability in change in the climatic variables between the 20 simulated grid points from the December–April period. Table 1 shows the monthly mean change in temperature, precipitation, dew point temperature and wind speed obtained by averaging the 20 grid points.

For SRES B2, the projected temperature increase in the study area ranges from 0.9 to 2.3 °C (mean change, 1.36 °C); under SRES A2, the increase ranges from 2.4 to 4.1 °C (mean change, 3.1 °C). December and January are predicted to experience the greatest warming under the B2 scenario, whereas a similar warming for all months is projected under SRES A2. Areas close to the main

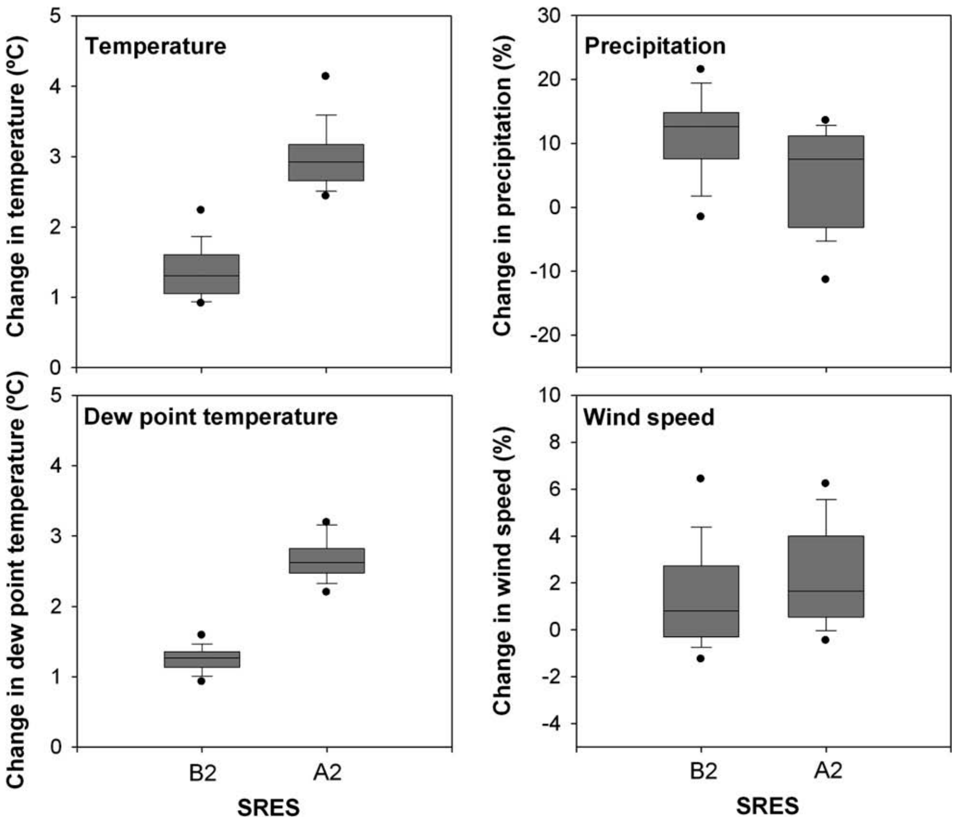

Fig. 8. Variability in projected change in temperature, precipitation, dewpoint temperature, and wind speed for 20 grid points.

divide (Spanish–French border) of the central-eastern Pyrenees are likely to undergo the most intense warming. The projected warming is more moderate with increasing distance to the main divide and reduced distance from the Atlantic Ocean.

On average, precipitation is projected to increase under SRES B2 (+11%) and remain largely stable under SRES A2 (−1.6%); however, these average values mask an important spatial variability: projected changes range from 22% to −2% for B2, and from +14% to −12% for A2. The most severe decrease in precipitation is projected for the southeastern part of the study area; precipitation in the north and northwestern sectors will remain unchanged or increase under both scenarios. Under the B2 scenario, the HIRHAM model predicts mean increases in precipitation of over 10% for December, January, and March; under the SRES A2, precipitation is simulated to increase in December and January, but decrease in February and March. Independently of the amount of precipitation, warmer temperatures will lead to more frequent events of liquid precipitation instead of snowfall with expected impacts on snowpack conditions within the study area.

The spatial distribution of projected changes in dew point temperature appears to be largely homogeneous across the Pyrenees, with generalized average increases of 1.2° and 2.6 °C for SRES B2 and A2, respectively. Wind speed under the future climate is projected to be similar to current conditions, with changes that barely exceed 5%.

Projected changes in snowpack by the end of the 21st century

Fig. 9 shows the simulated changes in ASWE according to climate change projected by the HIRHAM model under SRES B2 and A2 at different heights. The two contrasting emission scenarios lead to marked differences in simulated reductions of ASWE: the

Table 1
Change in monthly temperature, dew point temperature, precipitation and wind speed projected by HIRHAM model for SRES B2 and A2.

	SRES B2							SRES A2						
	November	December	January	February	March	April	May	November	December	January	February	March	April	May
T_a (°C)	2.5	2.1	1.7	1.3	0.5	1.2	2.7	3.2	3.1	3.1	3	3	3.3	3.5
T_d (°C)	2.2	1.9	1.6	0.7	0.8	1.2	2.1	2.8	3.4	2.8	2.6	1.8	2.2	2.7
P (%)	5.9	10.2	19.4	5.3	20.3	0.6	−18.6	−5.7	16.8	18.1	1.8	−4.9	−8.7	−28.5
W_s (%)	−3.1	−2.1	−0.9	2.7	5.6	1.5	−1.9	3.6	0.1	0.3	5.3	3.6	1.8	−2.3

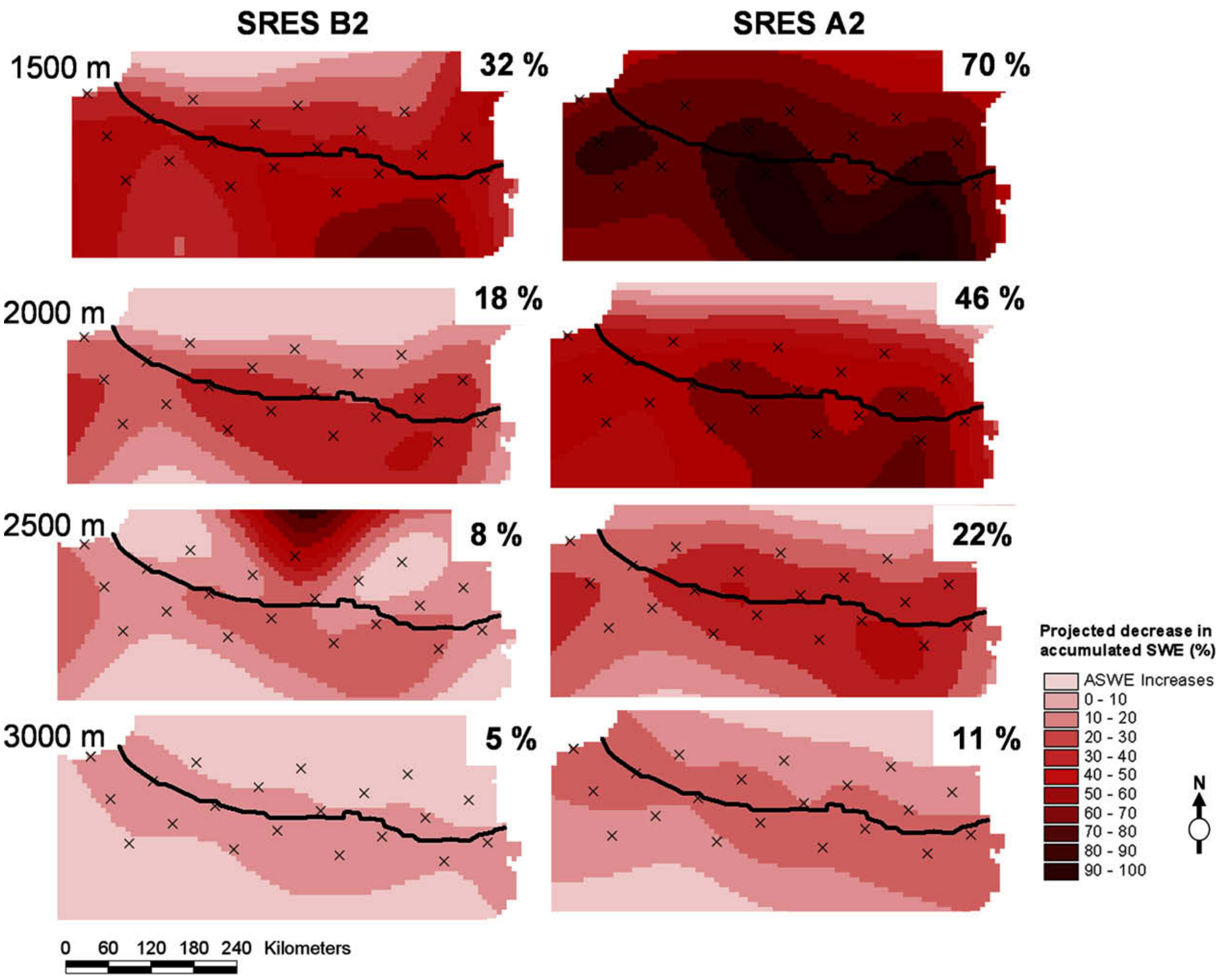

Fig. 9. Simulated changes in accumulated snow water equivalent according to climate change projected by the HIRHAM model under SRES B2 (left) and A2 (right) at different altitudinal planes: 1500 m a.s.l. (A), 2000 m (B), 2500 m (C), and 3000 m (D).

expected decrease under the A2 scenario is at least twice that projected under the B2 scenario. The impact of climate change on ASWE is characterized by strong altitudinal gradients and horizontal spatial variability. Under B2 conditions, ASWE is likely to decrease by an average of 32% at 1500 m a.s.l.; this figure increases to 70% under scenario A2. At 2000 m a.s.l., mean decreases in ASWE of 18% and 46% are simulated for the B2 and A2 scenarios, respectively. Areas above 2500 m a.s.l. are noticeably less affected by climate warming, with average decreases in ASWE of 8% and 22% according to B2 and A2, respectively; for the small areas located above 3000 m, the predicted decreases are again smaller, respectively, 5% and 11%.

Fig. 7 shows that warming will be more intense southward, and the maximum decrease in precipitation is projected to occur in the southeastern part of the region. Thus, it is not surprising to find that the impact of climate change on ASWE is greatest in the central and eastern parts of the Spanish Pyrenees, where the accumulation in SWE may decline by up to 90% at 1500 m a.s.l. under the A2 scenario, and up to 50% at 2500 m. Along the highest summits of the axial Pyrenees (above 3000 m), the decrease in SWE is expected to range between 7% and 15%, as snowpack located in the highest sectors close to the Spanish–French border (where peaks of this altitude are located) are expected to be the most exposed to climate change.

Fig. 10 is the same as Fig. 9, but for DSP. As with changes in ASWE, marked differences are found between the SRES B2 and A2 scenarios, and we observe the existence of horizontal variability, major impacts on southeastern areas, and altitudinal gradients. Under SRES B2, the decrease in DSP is expected to range between 44% at 1500 m a.s.l. and 11% at 3000 m. Under higher emissions (A2 scenario), the DSP is predicted to be half that under B2, with mean decreases of 78%, 49%, 23%, and 20% at 1500, 2000, 2500, and 3000 m a.s.l., respectively.

Fig. 11 shows the daily average (30 years and 20 points) evolution of snowpack during the control and SRES B2 and A2 scenarios. The snow curves show a general pattern of snow accumulation and melting during the year at the four considered altitudes. Because they represent the averages of a 30 year period and 20 points, the data show a smoother evolution than the typically irregular annual snowpack evolution observed at a given location. The figure highlights the dramatic decrease in snowpack simulated for the projected climate change likely to occur in coming decades. During the control period at 1500 m a.s.l., a thin but constant snowpack lasted from the beginning of December to the beginning of April; simulations for the future indicate that at this altitude snow will practically disappear under both climate change scenarios. At 2000 m a.s.l., a constant snowpack seems to remain during the winter months, with the possible existence of snowpack over the ground from mid-November to mid-May; however, it is noticeable thinner than that during the control period, and the simulated DSP falls from 218 days during the control period to 182 and 145 days for SRES B2 and A2, respectively. In addition, snowmelt will generally begin at the beginning of February, approximately 1 month earlier than currently. At 2500 m a.s.l., the impacts of climate

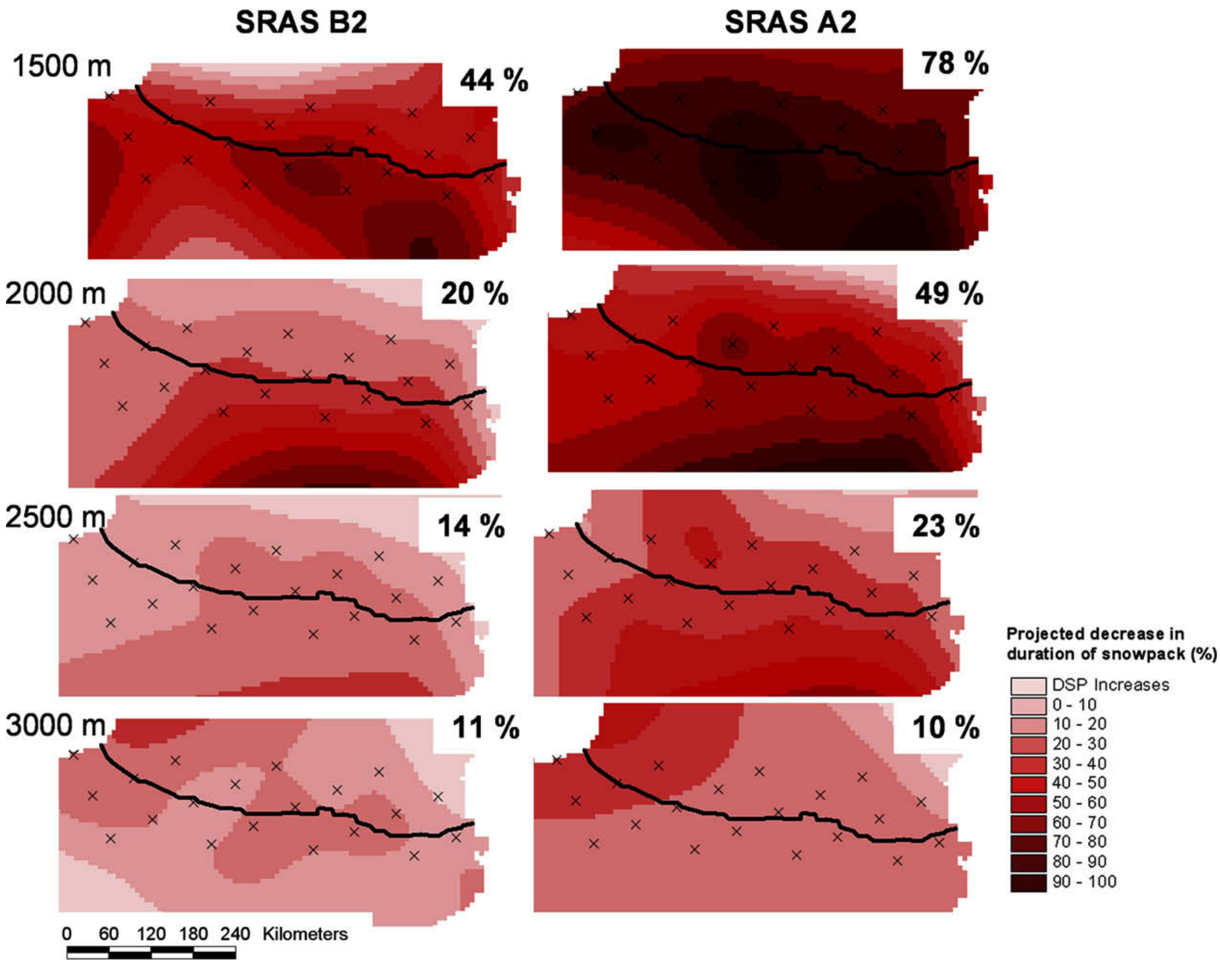

Fig. 10. Simulated changes in duration of snowpack according to climate change projected by the HIRHAM model under SRES B2 (left) and A2 (right) at different altitudinal planes: 1500 m a.s.l. (A), 2000 m (B), 2500 m (C), and 3000 m (D).

change on the general pattern of Pyrenean snowpack are reduced compared with those at lower altitudes, especially under B2 conditions. Under the A2 scenario, although the snowpack shows a clear evolution, it is affected by shifting climatic conditions. The DSP is reduced in 52 days, and the dominance of melting conditions may occur more than 1 month in advance of that of the present time. At 3000 m a.s.l., snowpack will remain in the future; however, the possibility of a perennial snow cover during the most favorable time of the year disappears under a greenhouse climate, and melting will occur 1 month in advance of that under current climatic conditions.

Discussion

SWE simulated by RCM-GCM has been used previously to analyze expected changes in snowpack over the coming decades at a very large scale (Räisanen, 2008); in other cases, data provided by RCM were successfully used as inputs for a multi-layer snow model, as used to estimate snow conditions in Finland at the end of the 21st century (Rasmus et al., 2004). In the present study, climatic variables from a RCM were adjusted to different altitudes to obtain reliable estimates of snow evolution in an area with complex climatic influences and heterogeneous topography. Aside from the expected biases and the inherent uncertainty resulting from the nature of the data used for validation, the scaling of data to altitudinal levels and the hourly disaggregation procedures, snowpack simulated using HIRHAM data adequately reflects changes in snowpack characteristics over the territory. Availability of RCM outputs at an hourly basis would noticeably simplify the methodological approach used in this study, as disaggregation to hourly would not be necessary. However, temporal resolution of most of the open source RCMs databases provide data at daily basis as maximum, and this work has demonstrated the reliability of snowpack information obtained after disaggregation procedure. Moreover, it is necessary to take into account that this study focused on computed changes, or "deltas"; this reduces the degree of potential uncertainty related to the quality of RCM outputs, as "deltas" are less sensitive to model errors (López-Moreno et al., 2008a).

This result suggests optimism regarding analyses of the impacts of climate change on various mountain sectors for which a lack of available meteorological records restricts the use of more common approaches, generally those based on a comparison of observed records with disturbed records according to delta factors. This latter procedure has been applied in analyzing the potential effects of climate change on snowpack in the Alps (Keller et al., 2005), Pyrenees (López-Moreno et al., 2008b), and Scandinavia (Mellander et al., 2007).

The lack of historical snow data is a common problem for many mountainous areas. Using downscaled information from RCMs, it is

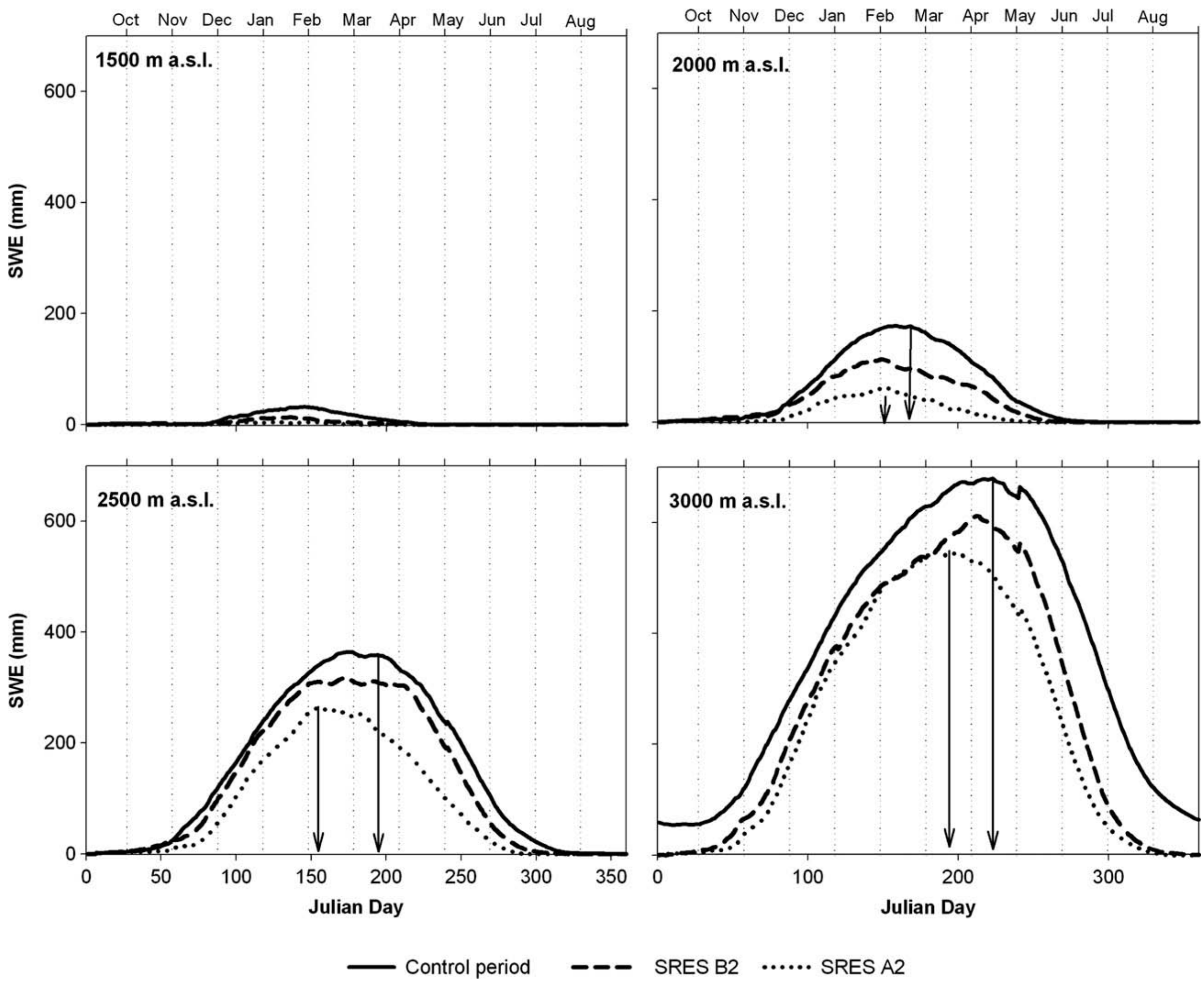

Fig. 11. Daily average (30 years and 20 points) evolution of snowpack during the control period and SRES B2 and A2 at four different heights. Arrows indicate the time from which melting becomes dominant.

not essential to compare output data with observational records; however, the availability of some observed snow and climate data is highly recommended to select the best model for simulating the climate of a given region, and to address the uncertainties related to climate simulations and snow modeling. Thus, for the Pyrenees, a previous analysis based on observations indicated that the HIRHAM model provides a reasonably good representation of climate in the area, with biases of less than 1 °C for temperature and 20% for precipitation (López-Moreno et al., 2008a).

In a previous investigation (López-Moreno et al., 2008b), the capability of GRENBLS in simulating snowpack from climate data of a single station (Izas station, 2060 m a.s.l.) was evaluated with success, and observations disturbed using delta factors enabled estimates of the following snow changes: maximum SWE will decrease by 50–60% and the duration of snowpack will decrease by around 2 months under the A2 scenario. These values are fully consistent with the changes obtained in the present study at 2000 m a.s.l. for the Spanish central Pyrenees. In the earlier study, nine different RCMs were tested, confirming that inter-model results shown relatively low variability and suggesting that model selection has only a limited effect on the obtained results.

The distributed approach followed in this study enables to conclude that changes in climate and snowpack at the end of the 21st century will be spatially heterogeneous throughout the study area. The present results highlight the complexity of mountainous areas in assessing spatial variability in the impact of climate change on climatic patterns, as documented previously in other mountain areas such as the Alps (Frei et al., 2006). The climate projections obtained for upcoming decades in the studied region are similar to those of previous studies that considered wider geographical areas, in particular Southwest Europe and the Western Mediterranean basin (Giorgi et al., 2004b; Gao et al., 2006; Nogués-Bravo et al., 2008); however, the scale employed in the present study enabled a detailed description of the spatial distribution of the predicted impacts, which may show marked changes over short distances.

In general, lower precipitation and warmer temperatures are expected for the central and southern (Spanish) side of the Pyrenees; thus, these are the sectors for which large decreases in snow accumulation and duration of snowpack are expected. The most pronounced impacts are predicted for the sector in the Pyrenees already most severely affected by water deficit. Here, snow plays an important role in releasing high and regular spring river flows to the main tributaries of the Ebro River, and climate change poses a serious threat to water management in the Ebro Valley (López-Moreno and García-Ruiz, 2004).

The HIRHAM model predicts that the main changes in snowpack are caused more by warmer temperatures than precipitation changes. It also explains the outstanding importance of altitudinal gradients in the simulated impacts of projected climate change on snowpack. Such vertical patterns have been detected in other mountainous sectors such as the Alps (Breiling and Charamza, 1999; Beniston et al., 2003), Scotland (Trivedi et al., 2007), and the Tarim Basin, China (Changchun et al., 2008). Summit areas appear little affected by climate change because temperature is largely below 0 °C for most of the year; however, most of the snow covered surface in the Pyrenees lies below 2500 m a.s.l., where a sharp decrease in thickness and duration of snowpack is expected. The simulations warn that the present-day continuous winter snow cover at 1500 m a.s.l. will become occasional; this may have important economic consequences, as most ski areas in the Pyrenees are located between 1500 and 2000 m a.s.l.

This work adds to the body of research that highlights the vulnerability of the ecology, hydrology, and economy of mountain systems and their surrounding areas to climate change; however, the magnitude of the impacts on snowpack may be reduced by half if a medium–low emission scenario is considered (B2) rather than maintaining the currently-increasing trends of gas concentration in the atmosphere that are likely to become consistent in time with the A2 scenario. This result is in line with other comparisons of the impacts predicted by different SRES (Maurer, 2007), highlighting the outstanding importance of the decisions to be made in the coming decades in terms of minimizing the impacts of climate change.

Conclusions

The Pyrenean snow accumulation and duration have been simulated with a surface energy balance model including an explicit snow module driving by hourly input data derived from daily outputs of the HIRHAM RCM. Daily data of twenty grid points of 50 km^2 was scaled to four representative elevation bands – 1500 m, 2000 m, 2500 m and 3000 m, and disaggregated into hourly-time step. This procedure enabled to simulate accumulated snow water equivalent (ASWE) and duration of the snowpack (DSP) at different altitudes for the control period (1960–1990) and the two greenhouse gas emission scenarios (A2 and B2, 2070–2100). The main conclusions derived from the analysis conducted in this study are as follows:

- Despite of the existence of biases related with RCM simulations, dissagregation of daily into hourly data, and scaling the punctual data in different altitudinal levels, a realistic representation of a snowpack series for the control period can be obtained by downscaling data from Regional Climate Models, the HIRHAM model in this case.
- Snowpack in the Pyrenees will be strongly affected by projected climate change in the region, with a marked decrease in ASWE and duration of snowpack; however, it is also necessary to consider the following points.
  - Different greenhouse gas emission scenarios (SRES) lead to marked differences in the severity of expected changes in snowpack, being at least twice as pronounced under the A2 scenario compared with B2.
  - Noticeable spatial differences in the magnitude of simulated changes in snowpack are detected. Snowpack in the central and eastern areas of the Spanish Pyrenees is clearly the most strongly affected by climate change.
  - The impact of climate change on snowpack is highly sensitive to the altitudinal gradient. The decrease in ASWE at 3000 m a.s.l. is just 25% of that simulated at 1500 m. In the latest sectors under SRES A2 and B2, ASWE is predicted to decrease by up to 78% and 44%, respectively, and DSP by 70% and 32%.

Acknowledgements

The study was supported by projects CGL 2004-04919-C02-01, CGL 2005-04508/BOS, and CGL2006-11619/HID funded by the Spanish Commission of Science and Technology, and the EU-FP7 ACQWA Project (FP7-ENV-2007-1-212250). The authors thank the PRUDENCE Project (http://prudence.dmi.dk) for free access to their collection of climate model outputs.

References

Anderson, E.A., 1973. National Weather Service River Forecast System – Snow Accumulation and Ablation Model. NOAA Tech. Mem. NWS Hydro 17, 217.
Anderson, E.A., 1976. A point energy balance model of a snow cover. Office of Hydrology, National Weather Service, NOAA Tech. Rep. NWS 19, 150 pp.
Barnett, T.P., Adam, J.C., Lettenmaier, D.P., 2005. Potential impacts of a warming climate on water availability in snow-dominated regions. Nature 438, 3003–3309.

Beniston, M., 1997. Variations of snow depth and duration in the Swiss Alps over the last 50 years: links to changes in large-scale climatic forcing. Climatic Change 36, 281–300.

Beniston, M., Keller, F., Koffi, B., Goyette, S., 2003. Estimates of snow accumulation and volume in the Swiss Alps under changing climatic conditions. Theoretical and Applied Climatology 76, 125–140.

Benoît, R., 1977. On the integral of the surface layer profile-gradient functions. Journal of Applied Meteorology 16, 859–860.

Berberan-Santos, M.N., Bodrenov, E.N., Pogliani, L., 1997. On the barometric formula. American Journal of Physics 65, 404–412.

Breiling, M., Charamza, P., 1999. The impact of global warming on winter tourism and skiing: a regionalised model for Austrian snow conditions. Regional Environmental Change 1 (1), 4–14.

Brun, E., Martin, E., Simon, V., Gendre, C., Coleou, C., 1989. An energy and mass balance model of snow cover suitable for operational avalanche forecasting. Journal of Glaciology 35, 333–342.

Brown, R., Bartlett, P., Mackay, M., Verseghy, D., 2006. Evaluation of snow cover in CLASS for SnowMIP. Atmosphere – Ocean 44, 223–238.

Carrivick, J.L., Brewer, T.R., 2004. Improving local estimations and regional trends of glacier equilibrium line altitudes. Geografiska Annaler 86a, 67–79.

Changchun, X., Yaning, C., Weihong, L., Yapeng, C., Hongtao, C., 2008. Potential impact of climate change on snow cover area in the Tarim River basin. Environmental Geology 53 (7), 1465–1474.

Christensen, J.H., Carter, T.R., Giorgi, F., 2002. PRUDENCE Employs New Methods to Assess European Climate Change, EOS, AGU, 83, 147.

Christensen, O.B., Christensen, J.H., Machenhauer, B., Botzet, M., 1998. Very high-resolution regional climate simulations over Scandinavia-present climate. Journal of Climate 11, 3204–3229.

Chueca-Cía, J., Julian-Andrés, A.M.A., López-Moreno, J.I., 2003. Variations of Glaciar Coronas, Pyrenees, Spain, during the 20th century. Journal of Glaciology 49 (164), 449–455.

Dankers, R., Christensen, O.B., 2005. Climate change impact on snow coverage, evapotranspiration and river discharge in the subarctic Tana basin, northern fennoscandinavia. Climatic Change 69, 367–392.

Dequé, M., Jones, R.G., Wild, M., Giorgi, F., Christensen, J.H., Hassell, D.C., Rockel, B., Jacob, D., Kjellström, E., de Castro, M., Kucharski, F., van der Hurk, F., 2005. Global high resolution versus Limited Area Model climate change projections over Europe: quantifying confidence level from PRUDENCE results. Climate Dynamics 25, 653–670.

Etchevers, P., Martin, E., Brown, R., Fierz, C., Lejeune, Y., Bazile, E., Boone, A., Dai, Y.J., Essery, R., Fernandez, A., Gusev, Y., Jordan, R., Koren, V., Kowalczyk, E., Nasonova, N.O., Olga, N., Pyles, R.D., Schlosser, A., Shmakin, A.B., Smirnova, T.G., Strasser, U., Verseghy, D., Yamazaki, T., Yang, Z.L., 2003. Validation of the energy budget of an alpine snowpack simulated by several snow models (SnowMIP project). Annals of Glaciology 38, 150–158.

Frei, C., Schöll, R., Fukutome, S., Schimidili, J., Vidale, P.L., 2006. Future change of precipitation extremes in Europe: intercomparison scenarios from regional climate models. Journal of Geophysical Research 111, D06105.

Gao, X., Pal, J.S., Giorgi, F., 2006. Projected changes in mean and extreme precipitation over the Mediterranean region from a high resolution doubled nested RCM simulation. Geophysical Research Letters 33, L03706.

García-Ruiz, J.M., Puigdefabregas, J., Creus, J., 1986. La acumulación de la nieve en el Pirineo Central y su influencia hidrológica. Pirineos 127, 27–72.

Giorgi, F., Bi, X., Pal, J.S., 2004a. Mean interannual variability and trends in a regional climate change experiment over Europe. I. Present-day climate (1961–1990). Climate Dynamics 22 (6/7), 733–756.

Giorgi, F., Bi, X., Pal, J.S., 2004b. Mean interannual variability and trends in a regional climate change experiment over Europe. II. Present-day climate (1961–1990). Climate Dynamics 23 (7), 839–858.

Jansson, P.E., Karlberg, L., 2004. Coupled heat and mass transfer model for soil–plant–atmosphere systems. Royal Institute of Technology, Department of Civil and Environmental Engineering, Stockholm, 435 pp. ftp://www.lwr.kth.se/CoupModel/CoupModel.pdf.

Hantel, M., Hirtl-Wielke, L.M., 2007. Sensitivity of Alpine snow cover to European temperature. International Journal of Climatology 27 (10), 1265–1275. doi:10.1002/joc.1472.

IPCC 2007. IPCC Fourth Assessment Report: The Physical Science Basis. Cambridge University Press, Cambridge, 996 pp.

Keller, F., Goyette, S., 2005. Snowmelt under different temperature increase scenarios in the Swiss Alps. In: Collins, David N., Roberto, Ranzi. (Eds.), Climate and Hydrology of Mountain Areas Carmen Dejong. Wiley, p. 315.

Keller, F., Goyette, S., Beniston, M., 2005. Sensitivity analysis of snow cover to climate change scenarios and their impact on plant habitats in alpine terrain. Climatic Change 72, 299–319.

Lasanta, T., Laguna Marín-Yaseli, M., Vicente-Serrano, S.M., 2007. Do tourism-based ski resorts contribute to the homogeneous development of the Mediterranean mountains? A case study in the Central Spanish Pyrenees? Tourism Management 28 (5), 1326–1339.

López-Moreno, J.I., García-Ruiz, J.M., 2004. Influence of snow accumulation and snowmelt processes on the distribution of streamflow in the central Spanish Pyrenees. Journal of Hydrological Sciences 49, 787–802.

López-Moreno, J.I., 2006. Cambio ambiental y gestión de embalses en el Pirineo Central Español. Consejo de Protección de la Naturaleza de Aragón. Zaragoza, 260 pp.

López-Moreno, J.I., Vicente-Serrano, S.M., 2007. Mapping of snowpack distribution over large areas using GIS and interpolation techniques. Climate Research 33, 257–270.

López-Moreno, J.I., Goyette, S., Beniston, M., 2008a. Climate change prediction over complex areas: spatial variability of uncertainties and expected changes over the Pyrenees from a set of regional climate models. International Journal of Climatology.

López-Moreno, J.I., Goyette, S., Beniston, M., Alvera, B., 2008b. Sensitivity of the snow energy balance to climatic changes: implications for the evolution of snowpack in the Pyrenees in the 21st century. Climate Research 36 (3), 203–217.

López-Moreno, J.I., Beniston, M., 2009. Daily intensity precipitation for the 21st century: seasonal changes over an Atlantic-Mediterranean gradient in the Pyrenean mountains. Theoretical and Applied Climatology 95, 375–384.

Marty, C., 2008. Regime shift of snow days in Switzerland. Geophysical Research Letters 35, L12501.

McFarlane, N.A., Boer, G.J., Blanchet, J.P., Lazare, M., 1992. The Canadian climate centre second generation general circulation model and its equilibrium climate. Journal of Climate 5, 1013–1044.

Mellander, P.E., Löfvenius, M.O., Laudon, H., 2007. Climate change impact on snow and soil temperature in boreal Scot pine stands. Climatic Change 85, 179–193. doi:10.1007/s-10584-007-9254-3.

Merritt, W., Alila, Y., Barton, M., Taylor, B., Cohen, S., Neilsen, D., 2006. Hydrologic response to scenarios of climate change in sub watersheds of the Okanagan basin, British Columbia. Journal of Hydrology 326, 79–108.

Mitasova, H., Mitas, L., 1993. Interpolation by regularized spline with tension. Mathematical Geology 25, 641–655.

Maurer, E.P., 2007. Uncertainty in hydrologic impacts of climate change in the Sierra Nevada Mountains, California under two emissions scenarios. Clim Change 82, 309–325.

Nakicenovic, N., Grübler, A., McDonalds, A., 1998. Global Energy Perspectives. Cambridge University Press, Cambridge. 299.

Nesje, A., Dahl, S.O., 2000. Glaciers and Environmental Change. Arnold Publishers, London.

Nogués-Bravo, D., Lasanta, T., López-Moreno, J.I., Araújo, M.B., 2008. Climate warming in Mediterranean mountains during the XXIst century. Ambio 37 (4), 280–285.

Nunez, M., Davies, J.A., Robinson, P.J., 1971. Solar Radiation and Albedo at a Lake Ontario Tower Site, Rept. No. HO.81276, Dept. of Geography, McMaster University, Hamilton, Ontario, 82 pp.

Outcalt, S.I., Goodwin, C., Weller, G., Brown, J., 1975. A Digital Computer Simulation of the Annual Snow and Soil Thermal Regimes at Barrow, Alaska. Cold Regions Research and Engineering Laboratory, Research Report 331, Hanover, NH, 18 pp.

Paltridge, G., Platt, C., 1976. Radiative Processes in Meteorology and Climatology. Developments in Atmospheric Science, No 5, Elsevier, 1976, Amsterdam, 318 pp.

Perry, R.H., Green, D.W., 1997. Perry's Chemical Engineers' Handbook, Seventh ed. McGraw-Hill. 2400.

Räisanen, J., 2008. Warmer climate: less or more snow. Climate Dynamics 30 (2–3), 307–319.

Rasmus, S., Räisänen, J., Lehning, M., 2004. Estimating snow conditions in Finland in the late 21st century using the SNOWPACK model with regional climate scenario data as input. Annals of Glaciology 38, 238–244.

Shallcross, D., 1997. Handbook of Psychometric Charts-humidity Diagrams for Engineers. Blackie Academic & Professional, London. 316 pp.

Stull, R.B., 1988. An Introduction to Boundary Layer Meteorology. Kluwer Academic Publishers, Dordrecht, Boston, London. 666 pp.

Trivedi, M.R., Browne, M.K., Berry, P.M., Dawson, T.P., Morecroft, M.D., 2007. Projecting climate change impacts on mountain snow cover in central Scotland from historical patterns. Arctic, Antarctic and Alpine Research 39 (3), 488–499.

Tuteja, N.K., Cunnane, C., 1997. Modelling coupled transport of mass and energy into the snowpack-model development, validation and sensitivity analysis. Journal of Hydrology 195 (1–4), 232–255.

Uhlmann, B., Goyette, S., Beniston, M., 2009. Sensitivity analysis of snow patterns in Swiss ski resorts to shifts in temperature precipitation and humidity under condition of climate change. International Journal of Climatology 29, 1048–1055.

Verseghy, D.L., 1991. CLASS – a Canadian land surface scheme for GCMs, I. Soil model. International Journal of Climatology 11, 111–133.